BL17SU
RIKEN Coherent Soft X-ray Spectroscopy

1. Introduction

As noted in the previous SPring-8/SACLA Annual Report FY2023, BL17SU has been operating as a beamline dedicated mainly to soft X-ray (SX) microspectroscopic studies over the last several years. Currently, more than 60% of the total user time at BL17SU, including public use, is dedicated to microspectroscopic experiments. While utilizing two existing spectromicroscopes, i.e., the versatile photoemission electron microscope (PEEM) [1,2] and the prototype apparatus of the scanning SX fluorescence spectromicroscope [3–9], as the main equipment, we have been operating the beamline together with adjusting a new scanning SX spectromicroscope with submicron spatial resolution and high counting efficiency. We have also been making efforts to realize a sophisticated angle-resolved photoelectron spectroscopy (ARPES) apparatus by developing an automatic measurement system.

2. Recent activities

As described in SPring-8/SACLA Annual Report FY2023, we have been developing a new scanning SX fluorescence spectromicroscope with submicron spatial resolution and high counting efficiency by

Table 1. Parameters of the focusing optics for the prototype apparatus.

	FZP–1	FZP–2
Membrane (material, thickness)	SiC, 100 nm	
Zone (material, thickness)	Au, 260 nm	
Outer diameter (μm)	910	1250
Outer most zone width (nm)	153	175
CBS*1 diameter (μm)	364	500
OSA*2 diameter (μm)	100	
Focusing distance (mm)	44.9 – 84.9	
Energy range E_{min} - E_{max}	designed (eV)	
1st order	400 – 756	260 – 450
3rd order	1200 – 2268	780 – 1350
Focused beam size	designed (nm)	
S2a*3=100 μm, E/ΔE*4～5,000	351 – 516	416 – 551
S2a=20 μm, E/ΔE～15,000	306 – 487	343 – 499
Focused beam size	measured (nm)	
S2a=20 mm, 1st order	about 329 @ 750 eV (FZP–1)	
S2a=40 mm, 1st order	about 257 @ 2,000 eV (FZP–1)	
S2a=100 mm, 3rd order	about 560 @ 1,200 eV (FZP–2)	
Diffraction efficiency	Photon flux (ph/s) (measured)	
1st order ～10.1%	8.1x10^8 @ 750 eV	1.2x10^9 @ 420 eV
3rd order ～1.1%	9.7x10^8 @ 1860 eV	6.8x10^8 @ 1000 eV

*1Center Beam Stop, *2Order Sorting Aperture, *3Exit slit, *4Resolving power

utilizing a monolithic Wolter mirror as a focusing component and multiple silicon drift detectors (SDDs) for the detection of the characteristic X-rays emitted from the sample surface. The previous version, i.e., the prototype apparatus, utilized the Fresnel zone plate (FZP) as the focusing component. Thus, the resultant available energy range and the focused SX-beam intensity were limited, as shown in Table 1. In the case of the FZP, its position in the focusing system must be adjusted each time the excitation energy is changed. In contrast, in the case of the Wolter mirror, no adjustment of the focusing system is required even when the excitation energy is changed. Furthermore, one of its advantages is that a more intense, focused beam can be expected, which in turn gives rise to high counting efficiency with multiple SDDs.

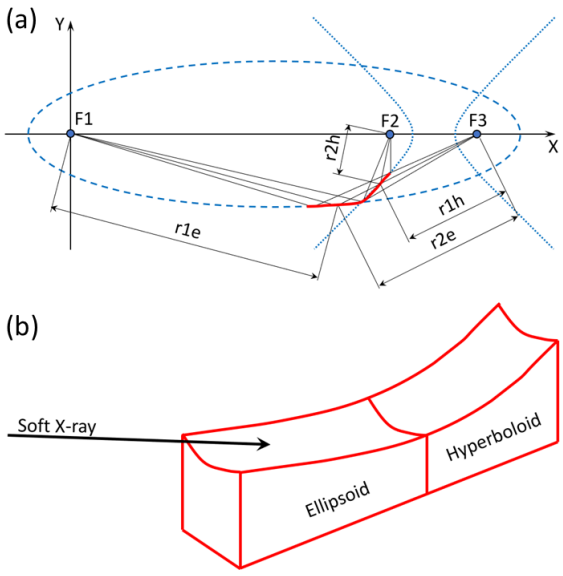

Fig. 1. (a) Optical layout and (b) schematic view of the monolithic Wolter mirror.

In Fig. 1, (a) an optical layout and (b) a schematic view of the monolithic Wolter mirror employed for the focusing component, which has an elliptical and a hyperbolic surface shape on a single substrate, of the new scanning SX fluorescence spectromicroscope are shown. One of the focal points of ellipsoid F1 is located at the source point. The SX-beam reflected by the ellipsoid is focused at the other focal point F3. The focal point of ellipsoid F3 coincides with that of the hyperboloid. The SX-beam reflected on the ellipsoid is finally focused at the other focal point F2 after reflecting on the hyperboloid. Table 2shows the parameters of the mirror. The present focusing component is designed to provide us with a focused beam size of about 500 nm. So far, we have achieved a beam size of 1.80 μm (H) x 0.85 μm (V) for the best focusing.

Table 2. Parameters of the monolithic Wolter mirror.

Shape	Monolithic Wolter
Substrate	SiO_2
Deflection of X-ray	Vertical
Outer dimensions (mm)	300 x 25 x 25 (L x W x T)
Useful area (mm)	280 x 5 (L x W)
Length of ellipsoid (mm)	151.8
Length of hyperboloid (mm)	128.2
Focal parameters	
Ellipsoidal part	
Incident angle (°)	1.0°
r1e (mm)	17491.803
r2e (mm)	896.787
Major axis (mm)	9194.295
Minor axis (mm)	69.122
Hyperboloidal part	
Incident angle (°)	1.0°
r1h (mm)	756.787
r2h (mm)	369.155
Major axis (mm)	193.816
Minor axis (mm)	9.225

As described in the SPring-8/SACLA Annual Report FY2023, the new apparatus can be used for microspectroscopic observations on various materials under the high vacuum conditions. In response, the role of the prototype apparatus will be changed to be specialized for the observation under the low vacuum condition (around 10 Pa) as well as for the observation of wet samples that require a He-atmosphere environment, where the vacuum and atmospheric pressure regions are separated using a membrane, *e.g.*, 1 mm x 1 mm x 0.2 μm (thickness) SiC or SiN, as a partitioning window.

Figure 2(a) shows a photograph of the outer view of the high-efficiency scanning SX fluorescence spectromicroscope under development. In this fiscal year, we are adjusting the monolithic Wolter mirror as the focusing component. In Fig. 2(b), we show the Wolter mirror mounted on the gyro, which has adjustment capabilities for the pitching, yawing, and rolling of the mirror block. Notably, up to six SDDs can be installed to detect fluorescent X-rays emitted from the sample. By increasing the number of SDDs, the solid angle can be increased, allowing for high-counting-efficiency measurements. Compared with the previous scanning SX spectromicroscope [3] operated with a single SDD, the spectromicroscope currently under development has a solid angle about 4.5 times larger. The reason why the solid angle does not increase more than sixfold is that the tips of the SDDs interfere with each other, preventing them from being placed too closely together. Fluorescent X-rays emitted from the sample are detected by SDDs placed at 45° from the incident light, and elemental mapping and X-ray absorption spectroscopy (XAS) by the partial fluorescence yield method can be performed.

Figures 3(a)–3(d) show observations of a permalloy ($Ni_{81}Fe_{19}$)/Si patterned sample prepared for a performance evaluation of the new apparatus. Figure 3(a) shows a secondary electron microscopy (SEM) image, where the approximate sizes of each

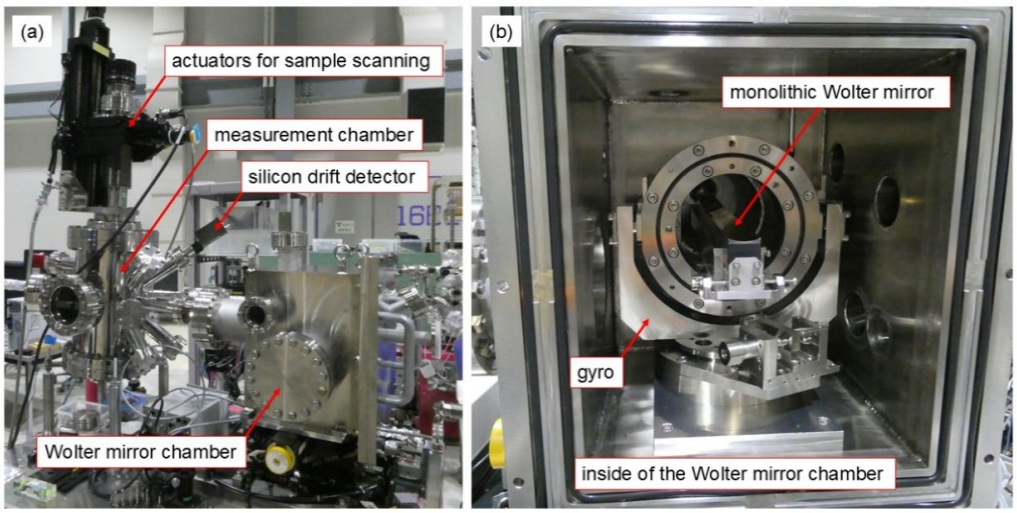

Fig. 2. (a) Photograph of the outer view of the high-speed scanning SX fluorescence spectromicroscope. (b) Photograph of the inner view of the Wolter mirror chamber. The monolithic Wolter mirror is mounted on the gyro.

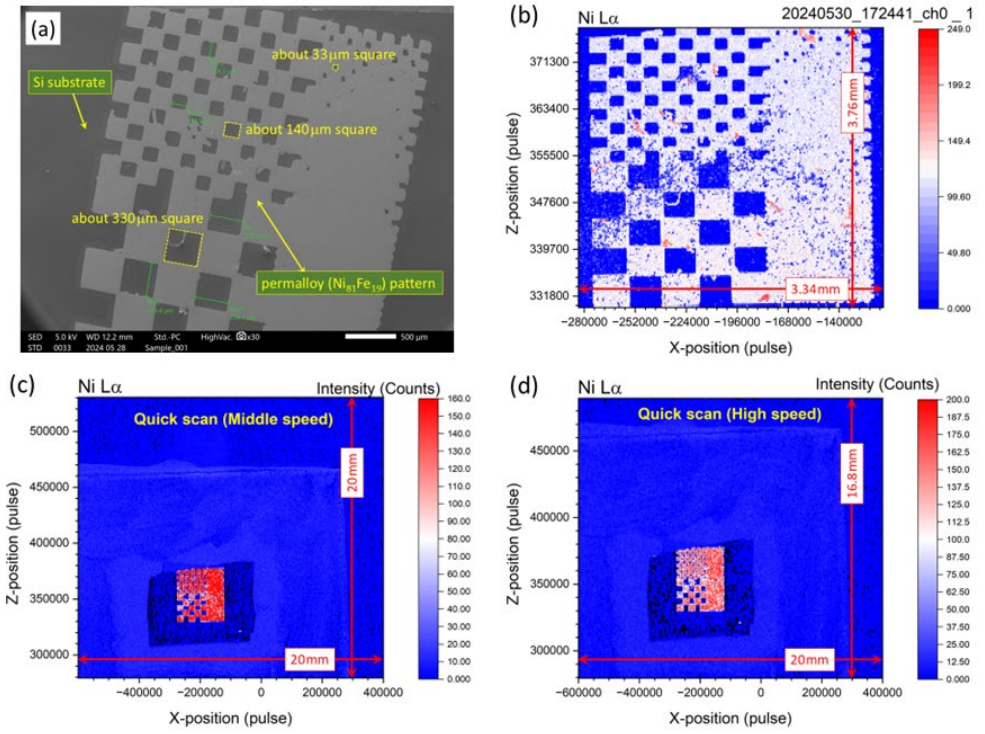

Fig. 3.(a) SEM image of the permalloy/Si patterned sample prepared for the evaluation of the new SX fluorescence spectromicroscope.

(b) Image of the patterned sample obtained using the new SX fluorescence spectromicroscope with step scan.

(c) Image of the patterned sample obtained using the new SX fluorescence spectromicroscope with quick scan (middle speed).

(d) Same as (c) with quick scan (high speed).

part of the pattern are indicated in the figure. Figure 3(b) shows an image of the same sample observed with the new scanning fluorescence spectromicroscope using a step scan over an area of 3.34 mm (H) × 3.76 mm (V). The pixel sizes were ΔX = 10 μm and ΔZ = 20 μm, giving a total of 63,315 pixels. With an integration time of 0.1 s per point, it took 890 minutes (14 h 50 min) to observe the entire image. For comparison, obtaining an equivalent image with the prototype apparatus requires 1 s integration time per point, resulting in about 44 hours of measurement. Figures 3(c) and 3(d) show the images of the same sample obtained using quick scans. Figure 3(c) was acquired while scanning at a medium speed, covering an area of 20 mm (H) × 20 mm (V) including the patterned region, with a total of 171,378 pixels and a measurement time of about 11 h 35 min. Figure 3(d) was acquired while scanning at a high speed, covering an area of 20 mm (H) × 16.8 mm (V) including the patterned region, with a total of 58,563 pixels and a measurement time of about 4 h 50 min.

The mapping data obtained by a quick scan have random coordinates, whereas those obtained by a step scan are aligned in a regular grid. This makes arithmetic operations between mappings straightforward. Therefore, a practical strategy is to first use a quick scan (high speed) to observe a wide

area of the sample, then progressively zoom in to expand the observation region, and finally perform a step scan to obtain a detailed mapping of the specific region of interest.

HAMAMOTO Satoru and OURA Masaki
Soft X-Ray Spectroscopy Instrumentation Team, Physical and Chemical Research Infrastructure Group, R&D of technology and systems for synchrotron radiation applications Division, RIKEN SPring-8 Center

References

[1] Ohkochi, T. Osawa, H. Yamaguchi, A. Fujiwara, H. & Oura, M. (2019). *Jpn. J. Appl. Phys.* **58**, 118001.

[2] Ohkochi, T. Tanaka, M. Ohtsuki, T. Horita, Z. Kitajima, F. Yamaguchi, A. Kotsugi, M. Ogawa, H. & Oura, M. (2023). *J. Electron Spectrosc. Relat. Phenom.* **267**, 147371.

[3] Oura, M. Ishihara, T. Osawa, H. Yamane, H. Hatsui, T. & Ishikawa, T. (2020). *J. Synchrotron Rad.* **27**, 664–674.

[4] Oura, M. Ishihara, T. & Yamaguchi, A. (2020). *Jpn. J. Appl. Phys.* **59**, 060902.

[5] Ishihara, T. Ohkochi, T. Yamaguchi, A. Kotani, Y. & Oura, M. (2020). *PLOS ONE* **15**, e0243874.

[6] Yamane, H. Oura, M. Takahashi, O. Ishihara, T. Yamazaki, N. Hasegawa, K. Ishikawa, T. Takagi, K. & Hatsui, T. (2021). *Commun. Mater.* **2**, 63.

[7] Yamane, H. Oura, M. Yamazaki, N. Ishihara, T. Hasegawa, K. Ishikawa, T. Takagi, K. & Hatsui, T. (2022). *Sci. Rep.* **12**, 16332.

[8] Oura, M. Takano, H. Hamamoto, S. Hatsui, T. Kurauchi, H. Okano, H. Kawaharada, M. Yokoyama, K. Yabashi, M. Akimoto, M. & Ishikawa, T. (2023). *J. Adhes. Sci. Technol.* **37**, 1737–1755.

[9] Yamaguchi, A. Ikeda, S. Nakaya, M. Kobayashi, Y. Haruyama, Y. Suzuki, S. Kanda, K. Utsumi, Y. Ohkochi, T. Sumida, H. & Oura, M. (2023). *J. Electron Spectrosc. Relat. Phenom.* **267**, 147385.